Challenge Journal of Structural Mechanics

Research Article

A comparative study on yield line mechanisms for four bolted extended end-plated connection

Yasin Onuralp Özkılıç [a,*]

[a] *Department of Civil Engineering, Necmettin Erbakan University, 42090 Konya, Turkey*

ABSTRACT

Extended end-plated connections are preferred in moment resisting frames due to their advantages such as no required in-situ welding, accurate fabrication and economic feasibility compared to flange welded moment connections. The capacity of the extended end-plated connections depends on bolt configurations, end-plate thickness, bolt diameter and their material properties excluding column part. The thickness of end-plate can be computed using yield line mechanisms. Different yield line patterns are available in the literature and some of these are adopted in seismic codes to estimate the thickness of end-plate. In this study, the accuracy of different yield line patterns is compared using collected experimental data and numerical analysis. A parametric numerical analysis was conducted utilizing the finite element tool, ABAQUS. The results of experimental data and parametric study were evaluated for both unstiffened and stiffened four bolted extended end-plated connections. The results revealed that the capacity of the end-plate connections significantly depends on the yield line mechanism. Therefore, selecting an accurate yield line mechanism is essential in order not to overestimate the thickness of the end-plate. More importantly is that these yield line mechanisms can be directly implemented to AISC 358 and Turkish Building Earthquake Code 2018 (TBEC-2018).

ARTICLE INFO

Article history:
Received 31 October 2020
Revised 31 January 2021
Accepted 2 March 2021

Keywords:
Extended end-plate connection
Stiffened
Unstiffened
Yield line mechanism
Numerical analysis

1. Introduction

End-plated connections are composed of a plate welded to a beam and attached to a beam or a column with pretensioned bolts. End-plated connections are classified into two categories: flush end-plate or extended end-plate. In extended end-plated connections, end-plates extend beyond the beam flanges so that at least one bolt row can be attached beyond the beam flanges. In flush end-plated connection, an extension of the plate is limited. Extended end-plated and flush end-plated connections are given in Fig. 1.

Extended end-plated connections are used in beam to column connections in moment-resisting frames. One of the most common extended end-plated configurations is shown in Fig. 2(a). In some cases, an additional plate is welded between end-plate and beam flanges. This plate is called stiffener or rib. This stiffener is used to reduce end-plate thickness. In other words, this stiffener is used to increase the moment capacity of the connection. Stiffened extended end-plated configurations are shown in Fig. 2(b).

End-plated connections are preferred due to eliminating welding process in field, easy and fast erection, cheap installation, and suitable for winter erection. Research related to end-plated connections has been studying since 1950 and the studies are still ongoing (Karasu and Vatansever, 2021; Akgönen and Güneş, 2017; Sağıroğlu, 2018; Yılmaz and Bekiroğlu, 2016; Özkılıç, 2021). The earlier connection designs result in thick end plates and large bolts since these designs were based on only statics. Later, design methods were developed thanks to finite element analyses. Other studies related to yield line theory improved the design methods.

Kennedy et al. (1981) developed design guidelines for tee sub connections including three stages of plate behavior: thick plate, intermediate plate and thin plate.

* *Corresponding author*. Tel.: +90-332-325-2024 ; E-mail address: yozkilic@erbakan.edu.tr (Y. O. Özkılıç)
ISSN: 2149-8024 / DOI: https://doi.org/10.20528/cjsmec.2021.02.005

In thick plates, no prying forces are available. When the load increase, plastic hinge occur in the plate and the prying forces are formed. The plate is called an intermediate plate when prying forces are present. If the prying forces reach maximum, the plate is called a thin plate.

Nomenclature

b_{fp}	Width of beam flange
b_p	Width of end-plate
C	Cyclic
d	Depth of beam excluding flange thickness
d_b	Bolt diameter
d_e	Vertical edge distance for outside holes
d_h	Sum of bolt hole diameters across width of end-plate
F_y	Yield strength of end-plate
F_u	Ultimate strength of end-plate
g	Horizontal distance between the bolts
h_o	Distance from the centerline of the compression flange to the tension side outer bolt row
h_i	Distance from the centerline of the compression flange to the tension side inner bolt row
L	Loading type
M	Monotonic
M_A	Moment capacity predicted by Adey et al. (1997)
M_S	Moment capacity predicted by Srouji et al. (1983)
$M_Ö$	Moment capacity predicted by Özkılıç (2020a)
M_u	Required flexural strength
p	The length of yield line which extends to web (0.35d)
p_{fi}	Vertical distance from inside of a beam tension flange to nearest inside bolt row
p_{fo}	Vertical distance from inside of a beam tension flange to nearest outside bolt row
Stif.	Stiffening
S	Stiffened
t_f	Flange thickness
t_p	End-plate thickness
t_s	Stiffener thickness
t_w	Weld thickness
U	Unstiffened
w_f	Flange weld thickness
w_s	Stiffener weld thickness
w_w	Web weld thickness

Murray (1988) reviewed previous studies for flush end-plated and extended end plated configurations and design guidelines were presented. Murray (1990) developed design procedures for unstiffened four bolt case and stiffened extended eight bolt case. Chasten (1992) conducted seven experiments with extended end plate connections. The effects of prying forces were investigated. A simple design guideline was presented in addition to the existing design procedure. Hendrick and others (1995) modified the Kennedy methods to predict bolt forces. The modified Kennedy methods were compared with experimental results. The results indicated that the modified Kennedy methods predict bolt forces accurately.

Borgsmiller (1995) developed new and simple design methods for flush end-plate and extended end plate connections. The bolt design methods were improved using Kennedy methods. The thickness of end-plates was determined using yield line theory. In previous test results, it was observed that prying forces should be taken into account when ninety percent of end-plate strength is achieved. If applied loads exceed 90% of plate strength, the end plate is considered as thin plate and if applied loads are less than 90% of plate strength, the end-plate is considered as thick plate. In thick plates, prying forces are neglected and in thin plates, prying forces are taken as maximum. This simplified method is used in the current AISC provision with slight changes.

Summer and Murray (2001) developed new design methods including thin and thick plate designs. Six test specimens designed according to these methods were tested under monotonic loading. The results indicated that proposed design methods conservatively predict the strength of connections. Summer and Murray (2002) tested seven extended end plate specimens under cycling loading. It was concluded that extended end plate connections can be used in seismic region and the connections should be stronger than the beam so that failure will occur in the beam section. Murray and Shoemaker (2002) published a new design procedure for flush end-plated and extended end-plated connections based on Borgimiller's (1995) study. However, these procedures were valid only for low seismic forces and wind. Thickness of end plates were determined from yield line analysis and bolt forces were determined from the simplified Kennedy method. Summer (2003) conducted experimental and analytical studies to develop design guidelines for eight bolted extended end-plated connections exposed to cyclic loading. Eleven specimens were tested under cyclic loading and nine specimens were tested under monotonic loading. The proposed design methods were compared with the previously tested ninety experiments. The proposed guideline was a good correlation with previous experimental results.

2. Yield Line Mechanisms

Yield line method was firstly developed in order to calculate the strength of concrete slabs. This method basically relies on the virtual work method. It is important to accurately determine failure patterns, in other words, yield lines. Inaccurate yield lines may result in conservative or unconservative results depends on the length of the yield line. This method is utilized for the calculation of end-plate resistance. End-plate fracture and bolt fracture are the main failure modes of the end-plated connection. The prediction of the moment capacity of the end-plate connection is calculated as virtual work produced by end-plate yield lines for yield mechanism.

Surtress and Man (1970) conducted the first study to predict the capacity of end-plate using yield lines. Then, Packer and Morris (1977) used yield line mechanism. Later, Mann and Morris (1979) modified the equation proposed by Packer and Morris. Whittaker and Walpole (1982) modified the yield line proposed by Surtress and

Man (1970) in order to take into account weld thickness. These yield lines are only applicable to unstiffened four bolted end-plated connections. Srouji et al. (1983) proposed yield line mechanisms for both unstiffened and stiffened four bolted end plated connections. This yield line mechanism is currently used by AISC 358. Two different yield lines were developed depends on the length of end-plate extension beyond the outside bolt line. The calculation of end-plate thickness is not related to diameter of bolts, instead, yield line pattern and yield strength of end-plates are only parameters that affect the thickness of end-plate. Different from Srouji et al. (1983), AISC 358 guideline includes a constant value of 1.11 to numerator.

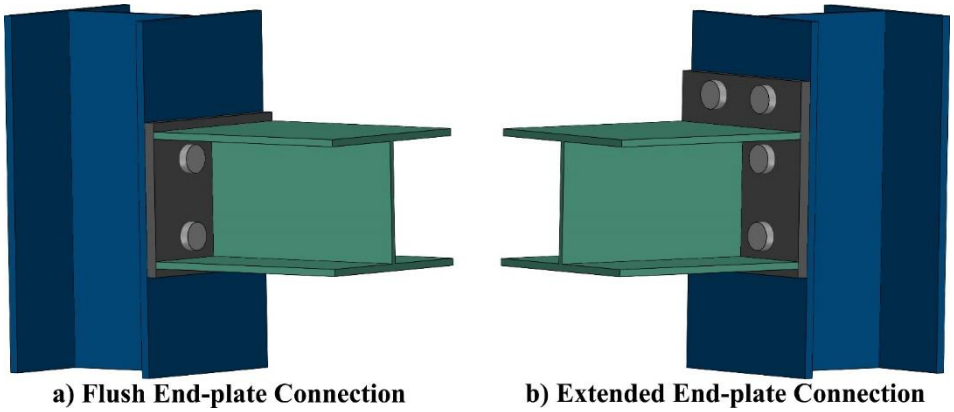

Fig. 1. End plated connections: (a) flush; (b) extended.

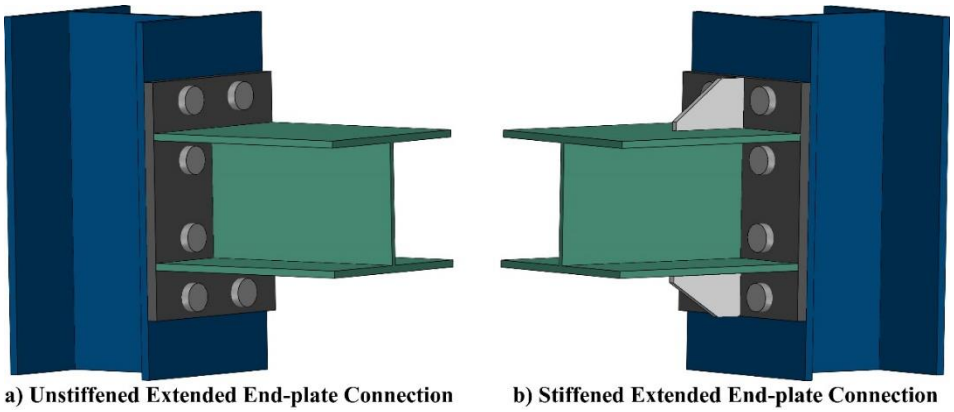

Fig. 1. Extended end plate connections: (a) Unstiffened; (b) Stiffened.

Adey et al. (1997) modified Whittaker and Walpole's yield line equations to obtain more accurate results for both unstiffened and stiffened four bolted end-plated connections. In the yield line mechanism of Whittaker and Walpole, yield line between the inner bolts reached 0.6d. However, Adey et al. (1997) changed the distance of this yield line to 0.35d. Moreover, the yield line mechanism of Whittaker and Walpole only takes into account weld thickness; however, the yield line mechanism of Adey et al. (1997) takes into account both weld thickness and diameter of bolt.

Özkılıç (2020a) and Özkılıç and Topkaya (2021a) proposed yield mechanism which takes into account reductions due to weld length and diameter of bolts for both unstiffened and stiffened four bolted end plated connection. Özkılıç (2020a) modified yield mechanism developed by Srouji et al. (1983) for unstiffened case while Özkılıç (2020a) modified yield mechanism developed by Shi et al. (2007) for stiffened case by taking into account reductions due to weld length and diameter of bolts.

The calculation of end-plate thickness using the aforementioned yield lines for unstiffened and stiffened four bolted cases are depicted in Tables 1 and 2, respectively. Moreover, the yield mechanisms proposed by Srouji et al. (1983), Aday et al. (1997) and Özkılıç (2020a) are illustrated in Fig. 3 for both unstiffened and stiffened four bolted cases.

Currently, Turkish Building Earthquake Code 2018 (TBEC-2018) defines four bolted extended end-plated connections as moment connections. However, the calculation of the capacity of the extended end-plated connections is not currently included in Turkish Building Earthquake Code 2018 (TBEC-2018). AISC 358-16 utilizes the yield mechanism of Srouji (1983) to calculate the end-plate thickness for four bolted extended end-plated connections which results in very conservative estimation.

In this present study, three different yield line mechanisms are evaluated using the collected experimental data and numerical analysis. The accuracy of these yield lines are compared and their conservatisms are presented. These yield lines can be directly adopted in TBEC-2018 and AISC 358-16 with proposed safety and overstrength factors.

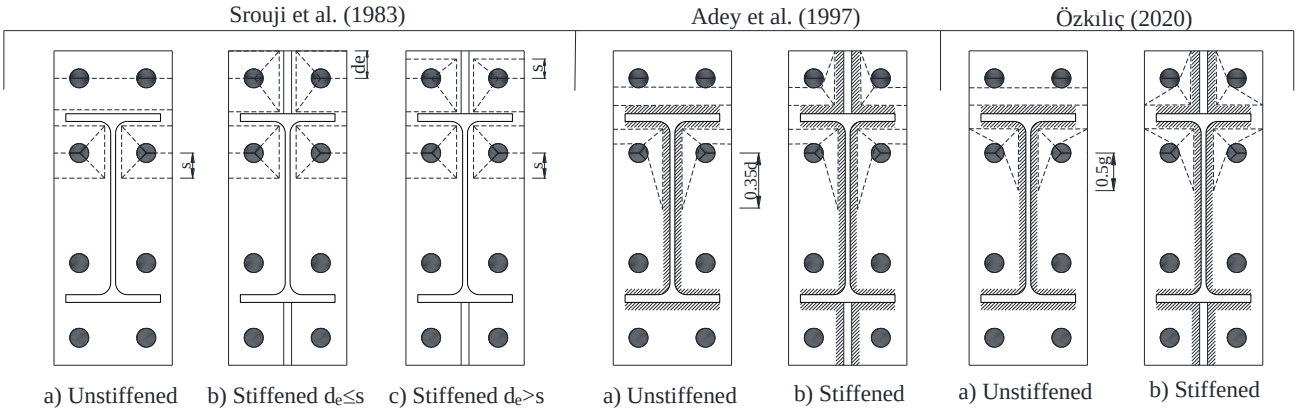

Fig. 3. Yield line mechanisms.

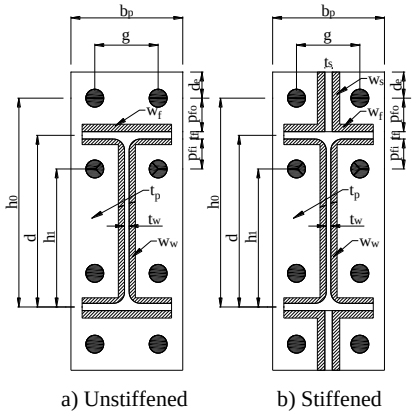

Fig. 4. Parameters used in the calculation of yield line mechanism.

Table 1. Calculation of end-plate thickness for unstiffened four bolted extended end-plate.

Surtress and Man (1970)	$t_{p,reqd} = \sqrt{\dfrac{M_u}{F_{py} d (2\dfrac{b_p}{c} + \dfrac{d_f}{g})}}$
Packer and Morris (1977)	$t_{p,reqd} = \sqrt{\dfrac{\alpha M_u}{F_{py} d (b_p - d_h)}}$
Mann and Morris (1979)	$t_{p,reqd} = \sqrt{\dfrac{\alpha M_u}{F_{py} d b_p}}$
Whittaker and Walpole (1982)	$t_{p,reqd} = \sqrt{\dfrac{M_u}{F_{py} d \left[2\dfrac{b_p}{c - t_f - w_f} + \dfrac{2p}{g - t_w - 2w_w}\right]}}$
Srouji et al. (1983)	$t_{p,reqd} = \sqrt{\dfrac{M_u}{F_{py} \dfrac{b_p}{2}\left[h_1\left(\dfrac{1}{p_{fi}} + \dfrac{1}{s}\right) + h_0\left(\dfrac{1}{p_{fo}}\right) - \dfrac{1}{2}\right] + \dfrac{2}{g}\left[h_1(p_{fi} + s)\right]}}$
Adey et al. (1997)	$t_{p,reqd} = \sqrt{\dfrac{M_u}{F_{py} d \left[\dfrac{b_p}{2(p_{fo} - \dfrac{d_b}{2} - w_f)} + \dfrac{2p}{g - t_b - 2w_w - d_b} + \dfrac{b_p - t_f - 2w_w}{2(p_{fi} - \dfrac{d_b}{2} - w_f)}\right]}}$
Özkılıç (2020a)	$t_{p,reqd} = \sqrt{\dfrac{M_u}{F_{py} \left[h_o\left[\dfrac{b_p}{2}\dfrac{1}{p_{fo} - 0.5d_b - w_f}\right] + 2h_1\left[\dfrac{b_p - t_{web} - 2w_w}{4(p_{fi} - 0.5d_b - w_f)} + \dfrac{p_{fi} - w_f + 0.5g}{g - t_{web} - 2w_w - d_b}\right]\right]}}$

Table 2. Calculation of end-plate thickness for stiffened four bolted extended end-plate.

Srouji et al. (1983)	when $d_e \le s$ $t_{p,reqd} = \sqrt{\frac{M_u}{F_{py}\left[\frac{b_p}{2}\left[h_1\left(\frac{1}{p_{fi}}+\frac{1}{s}\right)+h_0\left(\frac{1}{p_{fo}}+\frac{1}{2s}\right)\right]+\frac{2}{g}\left[h_1(p_{fi}+s)+h_0(p_{fo}+d_e)\right]\right]}}$ when $d_e > s$ $t_{p,reqd} = \sqrt{\frac{M_u}{F_{py}\left[\frac{b_p}{2}\left[h_1\left(\frac{1}{p_{fi}}+\frac{1}{s}\right)+h_0\left(\frac{1}{p_{fo}}+\frac{1}{s}\right)\right]+\frac{2}{g}\left[h_1(p_{fi}+s)+h_0(p_{fo}+s)\right]\right]}}$ $s = \frac{1}{2}\sqrt{b_p g}$
Adey et al. (1997)	$t_{p,reqd} = \sqrt{\frac{M_u}{F_{py} d\left[\frac{b_p - t_s}{2(p_{fo}-\frac{d_b}{2}-w_f)}+\frac{2(p_{fo}+d_e)}{g-t_s-2w_s-d_b}+\frac{2p}{g-t_b-2w_w-d_b}+\frac{b_p-t_f-2w_w}{2(p_{fi}-\frac{d_b}{2}-w_f)}\right]}}$
Özkılıç (2020a)	$t_{p,reqd} = \sqrt{\frac{M_u}{F_{py}\begin{bmatrix}2h_o\left[\frac{b_p-t_s-2w_s}{4(p_{fo}-0.5d_b-w_f)}+\frac{p_{fo}-w_f+d_e}{g-t_s-2w_s-d_b}\right]+\\ 2h_1\left[\frac{b_p-t_w-2w_w}{4(p_{fi}-0.5d_b-w_f)}+\frac{p_{fi}-w_f+0.5g}{g-t_{web}-2w_w-d_b}\right]\end{bmatrix}}}$

Currently, Turkish Building Earthquake Code 2018 (TBEC-2018) defines four bolted extended end-plated connections as moment connections. However, the calculation of the capacity of the extended end-plated connections is not currently included in Turkish Building Earthquake Code 2018 (TBEC-2018). AISC 358-16 utilizes the yield mechanism of Srouji (1983) to calculate the end-plate thickness for four bolted extended end-plated connections which results in very conservative estimation. In this present study, three different yield line mechanisms are evaluated using the collected experimental data and numerical analysis. The accuracy of these yield lines are compared and their conservatisms are presented. These yield lines can be directly adopted in TBEC-2018 and AISC 358-16 with proposed safety and overstrength factors.

3. Data Collection

The experimental data is collected for both the unstiffened and stiffened extended end-plated connections (Özkılıç and Topkaya, 2021b). The experimental data is selected based on two important criteria. The first criterion is that the main failure mode of the experiment should be end-plate related failure. Bolt failures, column failures, beam failures and welding failure may lead to making inaccurate interpretations for comparing the capacity of the end-plate. In other words, the specimens that failed due to non-related failures of end-plate are most probably failed before reaching the capacity of the end-plate. The second criterion is that the moment capacity of the beam section should be higher than the ultimate capacity of the experiment. This criterion is set in order to limit or prevent the contribution of the beam on the capacity. Similarly, if the capacity of the beam is much less than the ultimate capacity, the specimen is most probably failed before reaching the capacity of the end-plate.

The collected experimental data for the unstiffened case is shown in Table 3. A total of 34 experiments from 14 studies are selected based on the aforementioned criteria. Within the experimental data, the thickness of end-plate varies between 8 and 23 mm. Both cyclic and monotonic loadings are included. The diameter of bolt ranges between 12.7 mm and 31.8 mm. The depth of beams varies between 225 mm and 580 mm (except #26, 28).

The collected experimental data for the stiffened case is shown in Table 4. A total of 8 experiments from 4 studies are selected based on the aforementioned criteria. Unfortunately, very limited experiments are available accompanying the aforementioned criteria. Within the experimental data, the thickness of end-plate varies between 12-16 mm. Only cyclic loadings are available. The diameter of bolt ranges between 20.0 mm and 31.8 mm. The depth of beams varies between 225 mm and 580 mm.

4. Results and Discussions on the Collected Experimental Data

Two important capacities which are ultimate moment capacity (M_u) and plastic moment capacity (M_{pl}) are reported. The ultimate moment capacity (M_u) is the maximum moment that occurred during the experiments. On the other hand, plastic moment capacity (M_{pl}) is the moment at the intersection of tangent lines passing elastic and plastic zones. Fig. 5 demonstrates the typical moment rotation relationship for end-plated connection. The strength of the end-plated connection can be defined using M_u or M_{pl} and no absolute definition is available in the literature. It is accepted that all yield lines are formed at M_{pl}. Strain hardening and second order effects are included in M_u.

Table 5 shows the results for unstiffened extended end-plated connections. The ratio of M_p/M_u is equal or

larger than 1.0 indicating that the extended end-plate connection reached its ultimate capacities without reaching plastic moment capacity of the beam. The ratio of M_u/M_{pl} ranges between 1.05 and 2.11. It means that the extended end-plated connection can perform more than two times plastic moment capacity. It is a direct indication that design guidelines that utilize plastic moment capacities overly underestimate the capacity of the extended end-plate connection.

Table 3. Properties of experimented specimens for unstiffened four bolted case.

#	Specimens	L	t_p	F_y	F_u	d_b	t_f	t_w	b_{fp}	b_p	w_f	w_w	g	p_{fi}	p_{fo}	d_e	h_o	h_i
1	SP6	C	12	325	388	24	9.8	6.2	120	150	10	10	85	40	45	35	280	185
2	SP7	C	10	313	387	24	9.8	6.2	120	150	10	10	85	40	45	35	280	185
3	FS1a	M	10	340	481	20	10.7	7.1	150	150	6	4	90	40	40	30	335	245
4	FS1b	M	10	340	481	20	10.7	7.1	150	150	6	4	90	40	40	30	335	245
5	FS4a	M	10	698	741	20	10.7	7.1	150	150	6	4	90	40	40	30	335	245
6	FS4b	M	10	698	741	20	10.7	7.1	150	150	6	4	90	40	40	30	335	245
7	S2	C	13.3	295	501	25.4	11.6	7.2	171	200	10	10	100	44	44	30	390	290
8	S3	C	13	285	510	25.4	11.6	7.2	171	200	10	10	100	44	82	30	428	290
9	M1	C	15.9	340	510	28.6	19	11	193	230	12	12	125	45	45	60	500	390
10	M2	C	15.9	340	510	28.6	19	11	193	230	12	12	125	45	100	60	555	390
11	M3	C	19	356	504	31.8	19.0	11.4	193	230	12	12	125	45	100	60	555	390
12	L1	C	15.9	340	510	25.4	19.6	12	229	270	12	12	150	44	45	60	645	536
13	L2	C	15.9	340	510	25.4	19.6	12	229	270	12	12	150	45	135	60	735	535
14	L3	C	19	356	504	31.8	19.6	12	229	270	12	12	150	45	135	60	735	535
15	EPB 1-1	M	12	227	318	20	10.7	7	150	180	10	10	105	50	60	50	355	235
16	EPB 2-1	M	12	227	318	20	10.7	7	150	180	10	10	105	50	60	50	355	235
17	EP 1-1	M	12	227	318	20	10.7	7	150	180	10	10	105	50	60	50	355	235
18	EP 2-1	M	12	227	318	20	10.7	7	150	180	10	10	105	50	60	50	355	235
19	Beam10	M	10	331	506	20	10.2	6.1	180	180	10	6	100	58	58	50	357	237
20	Beam12	M	12	306	510	20	10.2	6.1	180	180	10	6	100	58	58	50	357	237
21	Jenkins	M	15	275	-	20	13.7	7.7	167	200	6	6	120	55	55	60	355	235
22	S10	M	10	425	567	24	11.8	6.7	166	270	8	5	140	40	40	36	341	249
23	EP-1-8	M	8	250	-	16	13.1	7.7	140	140	8	6	80	50	50	40	350	240
24	EP-3-10	M	10	250	-	16	13.1	7.7	140	140	8	6	80	50	50	40	350	240
25	EP-4-10	M	10	250	-	16	13.1	7.7	140	140	8	6	80	70	70	40	370	220
26	4E	C	13	427	-	22	12.7	9.5	203	203	6	6	102	64	38	57	1429	1314
27	E36	M	23	320	-	28.6	16.7	10	260	260	6	6	152	51	51	35	455	335
28	E55	M	19	408	-	25.4	25	16	205	205	6	6	127	102	35	45	1650	1405
29	P4	M	10	295	418	20	10.7	7.1	150	150	6	6	90	30	30	30	350	285
30	JD1	M	12	763	796	27	12	10	180	200	10	10	100	50	50	50	345	233
31	JD2	M	12	763	796	27	12	10	180	200	10	10	100	50	50	50	345	233
32	BC1-1	M	12	332	496	20	11.8	6.7	166	200	10	10	124	50	50	70	351	239
33	BCJ-2	M	12	332	496	20	11.8	6.7	166	200	10	10	124	50	50	70	351	239
34	BCJ-4	C	12	332	496	20	11.8	6.7	166	200	10	10	124	50	50	70	351	239

#1-2: Özkılıç (2020a); #3-6: Coelho et al. (2004); #7-14: Adey et al. (1997); #15-18: Bursi and Jaspart (1997); #19-20: Adegoke (2009); #21: Shi et al. (1996); #22: Zhu et al. (2019); #23-25: Arul Jayachandran et al. (2009); #26: Summer (2003); #27: Abel and Murray (1994); #28: Borgsmiller et al. (1995); #29: Aleksander and Damian (2019); #30-31: Qiang et al. (2018); #32-34: Wang et al. (2018)

Table 4. Properties of experimented specimens for stiffened four bolted case.

#	Specimens	L	t_p	F_y	F_u	d_b	t_f	t_w	b_{fp}	b_p	t_s	w_f	w_w	w_s	g	p_{fi}	p_{fo}	d_e	h_o	h_i
1	SP9	C	12	325	388	24.0	9.8	6.2	120	150	10	10	10	10	85	40	45	35	280	185
2	SP10	C	10	313	387	24.0	9.8	6.2	120	150	10	10	10	10	85	40	45	35	280	185
3	M4	C	15.9	340	510	31.8	19.0	11.4	193	230	19	10	10	10	125	50	100	60	560	395
4	M6	C	15.9	340	510	31.8	19.0	11.4	193	230	19	10	10	10	125	50	100	60	560	395
5	L4	C	15.9	340	510	31.8	19.6	11.9	229	270	19	12	12	12	150	45	135	60	735	535
6	4ES	C	13	386	601	25.4	9.5	6.4	203	203	6	6	5	6	114	45	45	44	586	507
7	JC4	C	16	282	588	20.0	12.0	8.0	200	200	8	10	10	10	108	50	50	50	344	232
8	JC5	C	12	318	611	20.0	12.0	8.0	200	200	8	10	10	10	108	50	50	50	344	232

#1-2: Özkılıç (2020a); #3-5: Adey et al. (1997); #6: Ryan (1999); #7-8: Bu et al. (2019)

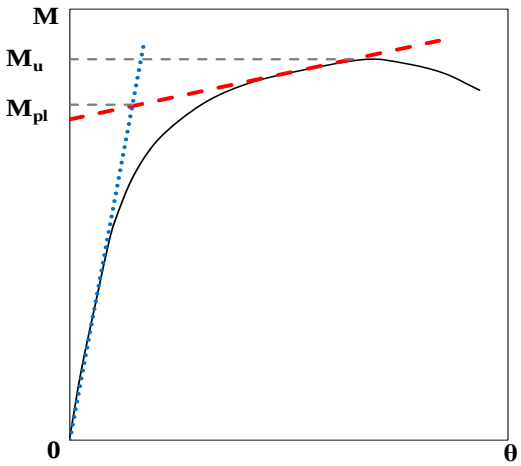

Fig. 5. Typical moment-rotation relationship.

Fig. 6 shows the comparison of the predicted and actual plastic moment capacities. The average ratios of actual plastic and predicted moment capacities are 1.27, 0.84 and 0.96 according to yield mechanisms of Srouji et al. (1983), Adey et al. (1997) and Özkılıç (2020a), respectively. The accuracy of the latter is better than those of formers. Except for three test specimens, the yield mechanism of Srouji et al. (1983) underestimates the plastic moment capacity. On the other hand, the yield mechanism of Adey et al. (1997) overestimates the plastic moment capacities except for 10 test specimens. It should also be mentioned that the yield mechanism of Adey et al. (1997) significantly overestimates plastic moment capacities of #14, 26 and 28 where the depth of the beam is relatively higher. This behavior is expected since the yield mechanism of Adey et al. (1997) extends the yield line up to 0.35 times the depth of the beam. Compared to those yield line mechanisms, the results of the yield line mechanism proposed by Özkılıç (2020a) give more balanced results.

The average ratio of ultimate moment capacity to moment capacity calculated using the yield line mechanism proposed by Srouji et al. (1983) is 1.92. The maximum ratio can reach 2.84, which is a significant underestimation of the ultimate capacity. The average ratios modify to 1.30 and 1.47 for the yield line mechanism proposed by Adey et al. (1997) and Özkılıç (2020a). The fact that the minimum ratio of ultimate moment capacity to moment capacity calculated using the yield line mechanism proposed by Srouji et al. (1983) is 1.03 indicates that for all cases this yield mechanism gives conservative results. The ratio of ultimate moment capacities to moment capacity predicted by Adey et al. (1997) for #14, 26 and 28 is significantly low due to the depth of the beam.

The relation between end-plate thickness and the ratio of actual ultimate and predicted moment capacities is shown in Fig. 7. It is seen that only for two cases the ratio is higher than 2.0 for the cases where thickness of end-plate is higher than 12 mm. On the other hand, the highest ratio is observed when the thickness of end-plate is 8 mm.

Table 6 shows the results for stiffened extended end-plated connections. Due to the very limited availability of experimental data for the stiffened case, the cases where the ratio of M_p/M_u is higher than 0.75 are also utilized provided that the main failure is related to the end-plate. The ratio of M_u/M_{pl} ranges between 1.46 and 1.93. A similar conclusion can be drawn also here that the stiffened extended end-plated connection can perform up to almost two times plastic moment capacity. The average ratios of predicted and actual plastic moment capacities are 1.16, 0.87 and 0.87 according to the yield mechanisms of Srouji et al. (1983), Adey et al. (1997) and Özkılıç (2020a), respectively. The prediction of Özkılıç (2020a) is slightly better than the others. This can also be seen in Fig. 8. On the other hand, the average ratios of ultimate plastic moment capacities and predicted capacities are 1.99, 1.36 and 1.48 according to the yield mechanisms of Srouji et al. (1983), Adey et al. (1997) and Özkılıç (2020a), respectively.

5. Numerical Study

Numerical study was conducted in order to evaluate further the prediction of the yield line mechanism for the parameters which did not particularly examined in the collected experimented specimens given in the previous section. Numerical analyses were performed using the finite element tool, ABAQUS. The experimental program conducted by Zhu et al. (2019) was adapted. After the verification model, a parametric study was carried out. Nonlinear geometry and material were considered. C3D8R type of elements was utilized for meshing all

members. The end-plate was divided into four elements through the thickness, which was recommended by Özkılıç (2020b) in order to simulate the bending and buckling behavior accurately. Mesh sizes of 10 and 5 mm were utilized for the end-plate and bolts whereas a slightly larger mesh size of 20 mm was used for the beam and column face. The column was not modeled explicitly; instead, the column face was modeled in order to reduce computational cost. The welds were explicitly implemented in the model. Mesh configuration is depicted in Fig. 9. All degrees of freedom of the bottom surface of the column face were restrained. Loading was applied to the end of the beam where MPC constraint was defined. The finite sliding surface-to-surface contact with tangential contact behavior was defined to model contact between bolts and end-plate and between end-plate and the column face. The bolts were pre-tensioned using "Bolt Load" option in ABAQUS.

Table 5. Results for unstiffened extended end-plated connections.

#	M_{pl}	M_u	M_p	M_p/M_u	M_u/M_{pl}	M_S	M_A	$M_{\bar{O}}$	M_{pl}/M_S	M_{pl}/M_A	$M_{pl}/M_{\bar{O}}$	M_u/M_S	M_u/M_A	$M_u/M_{\bar{O}}$
1	75	138	147	1.06	1.84	68	115	106	1.11	0.65	0.71	2.04	1.20	1.30
2	55	116	147	1.27	2.11	45	77	71	1.21	0.72	0.77	2.56	1.51	1.63
3	106	142	189	1.33	1.34	66	90	83	1.61	1.17	1.28	2.16	1.57	1.71
4	109	161	189	1.17	1.48	66	90	83	1.65	1.21	1.31	2.44	1.78	1.94
5	166	185	189	1.02	1.11	135	185	170	1.23	0.90	0.97	1.37	1.00	1.09
6	164	188	189	1.00	1.15	135	185	170	1.21	0.88	0.96	1.39	1.01	1.10
7	180	203	327	1.61	1.13	135	233	208	1.33	0.77	0.87	1.50	0.87	0.98
8	140	191	327	1.71	1.36	107	167	139	1.30	0.84	1.01	1.78	1.14	1.37
9	460	700	761	1.09	1.52	298	590	520	1.54	0.78	0.89	2.35	1.19	1.35
10	255	483	761	1.58	1.89	246	422	340	1.04	0.60	0.75	1.96	1.14	1.42
11	320	596	761	1.28	1.86	579	674	541	0.55	0.48	0.59	1.03	0.88	1.10
12	520	774	1310	1.69	1.49	437	838	719	1.19	0.62	0.72	1.77	0.92	1.08
13	344	551	1310	2.38	1.60	337	558	432	1.02	0.62	0.80	1.64	0.99	1.27
14	385	742	1310	1.77	1.93	504	938	731	0.76	0.41	0.53	1.47	0.79	1.01
15		94	272	2.89		58	75	69				1.63	1.26	1.36
16		96	169	1.76		58	75	69				1.67	1.28	1.39
17		120	168	1.40		58	75	69				2.08	1.61	1.74
18		98	168	1.71		58	75	69				1.70	1.31	1.42
19	80	158	216	1.37	1.98	61	75	70	1.32	1.07	1.15	2.60	2.12	2.27
20	96	155	216	1.39	1.61	81	99	93	1.19	0.97	1.04	1.92	1.56	1.67
21	150	198	233	1.18	1.32	114	128	126	1.32	1.17	1.19	1.74	1.54	1.57
22	152	245	252	1.03	1.61	91	180	137	1.67	0.84	1.11	2.69	1.36	1.78
23	43	80	143	1.79	1.86	28	38	33	1.53	1.14	1.32	2.84	2.12	2.46
24	61	112	143	1.28	1.84	44	59	51	1.39	1.03	1.20	2.54	1.90	2.20
25	52	96	143	1.49	1.85	39	49	43	1.34	1.06	1.20	2.47	1.95	2.21
26	850	1229			1.45	775	2193	986	1.10	0.39	0.86	1.59	0.56	1.25
27	476	681	1365	2.00	1.43	506	655	656	0.94	0.73	0.73	1.35	1.04	1.04
28	1836	1928	10002	5.19	1.05	1835	4917	2734	1.00	0.37	0.67	1.05	0.39	0.71
29	138	151	192	1.27	1.09	74	130	117	1.86	1.06	1.18	2.04	1.16	1.29
30	313	406	620	1.53	1.30	225	352	332	1.39	0.89	0.94	1.80	1.15	1.22
31	320	394	620	1.57	1.23	225	352	332	1.42	0.91	0.96	1.75	1.12	1.19
32	97	176	246	1.40	1.81	92	118	115	1.06	0.82	0.84	1.92	1.49	1.53
33	118	194	246	1.27	1.64	92	118	115	1.29	1.00	1.03	2.12	1.64	1.69
34	132	204	246	1.21		92	118	115	1.44	1.11	1.15	2.23	1.72	1.77
Mean	273	353	714	1.60	1.55	228	442	313	1.27	0.84	0.96	1.92	1.30	1.47
Min	43	80	143	1.00	1.05	28	38	33	0.55	0.37	0.53	1.03	0.39	0.71
Max	1836	1928	10002	5.19	2.11	1835	4917	2734	1.86	1.21	1.32	2.84	2.12	2.46

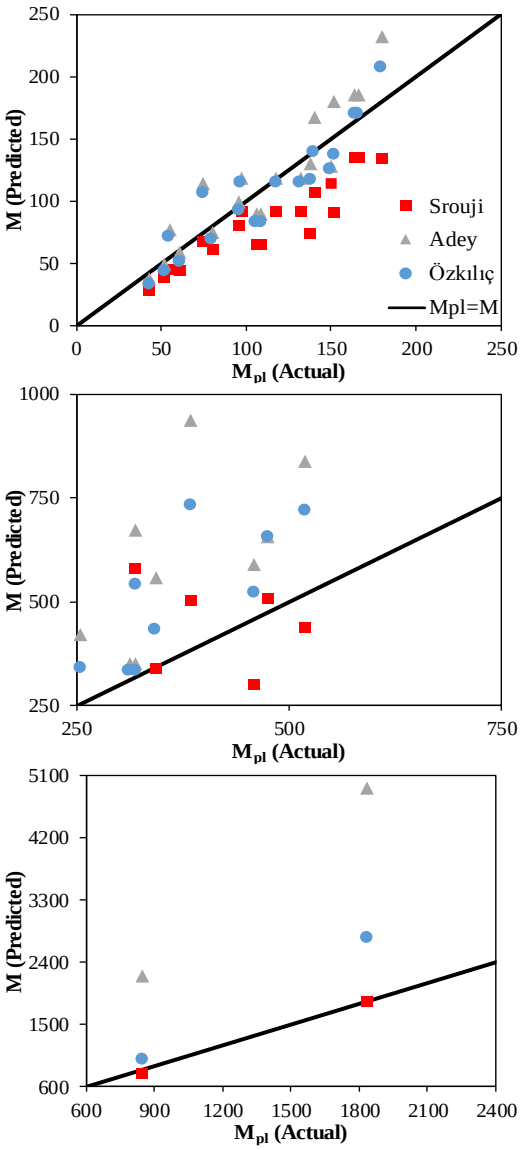

Fig. 6. The comparison of actual and predicted moment capacities for unstiffened cases.

In order to verify the assumed boundary conditions, mesh configuration and material model, the specimen S10BP of the study performed by Zhu et al. (2019) was simulated. This specimen is the same as with #22 specimen in Table 3 except that a backing plate was included, which resulted in an increase in the rigidity of the column face. For the verification model, the material properties of the specimen given by Zhu et al. (2019) were used. Fig. 10 compares the experimental findings and numerical results in terms of moment-rotation. It is observed that the numerical models exhibit slightly rigid behavior. This can be attributed to the behavior of the column which may act inelastic during the experiments. However, very slight differences of 4% and 5% between numerical and experimental results were observed for M_u and M_{pl} capacities, respectively. Fig. 11 demonstrates the failure mode at the end of the experiment at 0.10 rad rotation and PEEQ distribution at 0.10 rad rotation. In numerical models, high strain concentration was observed at the edge of the flange where failure was observed in the experiments. Moreover, the numerical model exhibited similar deformed shapes with the experimented specimen. Therefore, it can be concluded that a good agreement is observed between numerical and experimental findings.

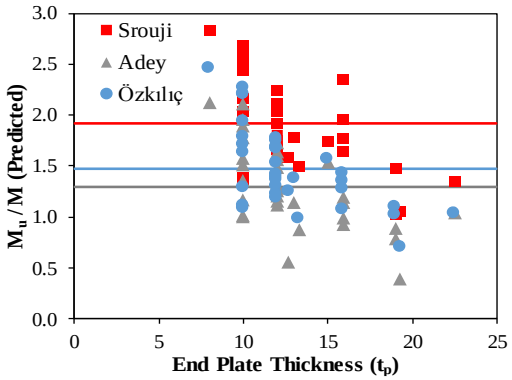

Fig. 7. The ratio of actual ultimate and predicted moment capacities.

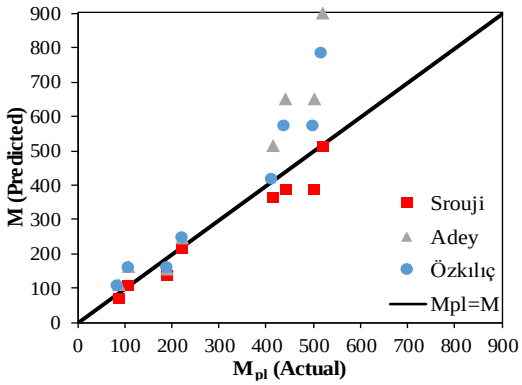

Fig. 8. The comparison of actual and predicted moment capacities for stiffened cases.

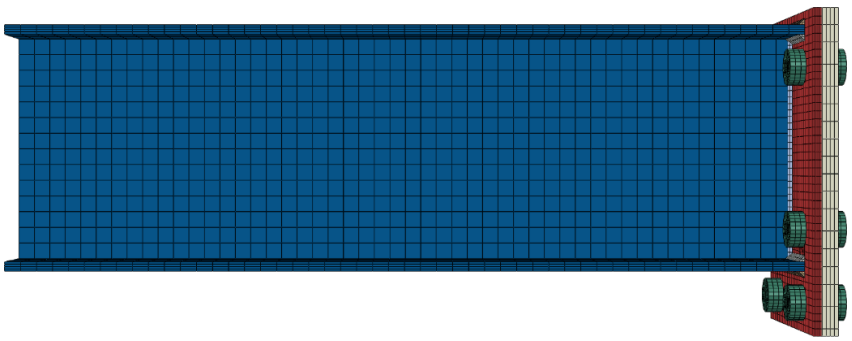

Fig. 9. Mesh configuration.

Table 6. Results for stiffened extended end-plated connections.

#	M_{pl}	M_u	M_p	M_p/M_u	M_u/M_{pl}	M_S	M_A	$M_Ö$	M_{pl}/M_S	M_{pl}/M_A	$M_{pl}/M_Ö$	M_u/M_S	M_u/M_A	$M_u/M_Ö$
1	109	191	147	0.77	1.75	104	165	157	1.04	0.66	0.69	1.83	1.16	1.22
2	87	168	147	0.87	1.93	70	110	105	1.25	0.79	0.83	2.41	1.53	1.60
3	502	734	761	1.04	1.46	386	654	569	1.30	0.77	0.88	1.90	1.12	1.29
4	440	796	761	0.96	1.81	386	654	569	1.14	0.67	0.77	2.06	1.22	1.40
5	520	999	1310	1.31	1.92	512	901	784	1.02	0.58	0.66	1.95	1.11	1.27
6	414	623	716	1.15	1.50	364	516	415	1.14	0.80	1.00	1.71	1.21	1.50
7	222	362	268	0.75	1.63	218	247	246	1.02	0.90	0.90	1.66	1.46	1.47
8	191	331	268	0.81	1.73	138	157	156	1.38	1.22	1.22	2.39	2.11	2.12
Mean	311	526	547	0.96	1.72	272	425	375	1.16	0.80	0.87	1.99	1.36	1.48
Min	87	168	147	0.74	1.46	70	110	105	1.02	0.58	0.66	1.66	1.11	1.22
Max	520	999	1310	1.31	1.93	512	901	784	1.38	1.22	1.22	2.41	2.11	2.12

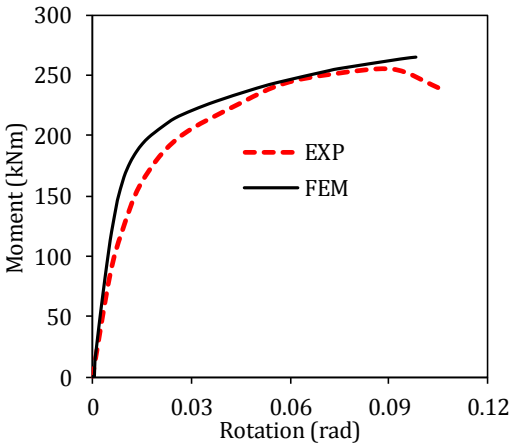

Fig. 10. Comparison of moment-rotation curves.

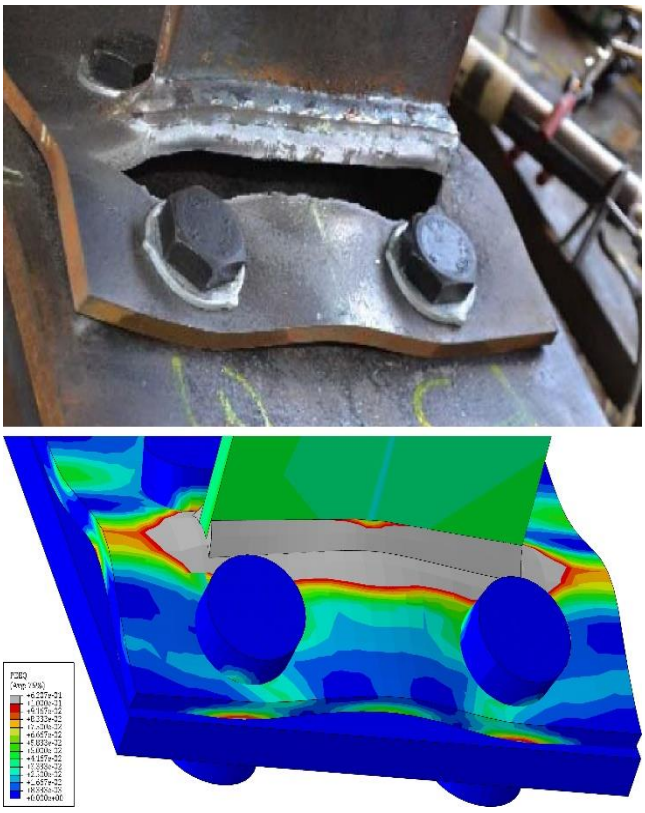

Fig. 11. Comparison of failure modes.

After the verification of the numerical model, a parametric study was conducted. The main aim of the parametric study was to explore the effects of the parameters on the accuracy of the yield line mechanisms. These parameters were selected based on the collected experimental data. The parameters which were not emphasized during the experiments were included in the parametric study. The parametric study was conducted for unstiffened and stiffened cases. A total of twenty models given in Table 7 were constructed. Models 1-10 were built for unstiffened cases whereas Models 11-20 were constructed for stiffened cases. Models 1 and 11 represent the reference models. Diameters of bolt were increased to 30 mm for Models 2 and 12. Gage distance was decreased to 100 mm for Models 3 and 13. Thickness of weld was double for Models 4 and 14. For Models 5 and 15, depth of beam was increased. Edge distance was increased to 60 mm for Models 6 and 16. Width of beam flange was increased to 250 mm for Models 7 and 17. Vertical distance from inside of a beam tension flange to nearest inside bolt row was reduced to 35 mm for Models 8 and 18 whereas vertical distance from inside of a beam tension flange to nearest outside bolt row was decreased to 35 mm for Models 9 and 19. Thickness of end-plate was reduced to 8 mm for Models 10 and 20.

In the parametric study, the negative contribution of the beam, column and bolts to the capacity was eliminated. This was achieved by avoiding any failure or yielding of the bolts, beam and columns. Pursuant to this goal, yield strength of 235 MPa and 420 MPa were selected for the end-plate and beam, and the column face was modeled as elastic. Moreover, a slightly larger bolt diameter of 27 mm with 10.9 Grade was selected. The multilinear stress-strain curve recommended by Yun and Gardner (2017) was employed. Isotropic hardening was implemented to simulate the material model. The numerical modes were loaded up to 0.10 rad rotation which is the rotation capacity of the experimented specimen.

Table 7. Properties of experimented specimens for unstiffened four bolted case.

#	*Stif.*	t_p	d_b	t_f	t_w	b_{fp}	b_p	w_f	w_w	g	p_{fi}	p_{fo}	d_e	h_o	h_i
1	U	10	27	11.8	6.7	166	270	8	5	140	40	40	36	341	249
2	U	10	30	11.8	6.7	166	270	8	5	140	40	40	36	341	249
3	U	10	27	11.8	6.7	166	270	8	5	100	40	40	36	341	249
4	U	10	27	11.8	6.7	166	270	16	10	140	40	40	36	341	249
5	U	10	27	11.8	6.7	166	270	8	5	140	40	40	36	541	449
6	U	10	27	11.8	6.7	166	270	8	5	140	40	40	60	341	249
7	U	10	27	11.8	6.7	250	270	8	5	140	40	40	36	341	249
8	U	10	27	11.8	6.7	166	270	8	5	140	35	40	36	341	254
9	U	10	27	11.8	6.7	166	270	8	5	140	40	35	36	336	249
10	U	8	27	11.8	6.7	166	270	8	5	140	40	40	36	341	249
11	S	10	27	11.8	6.7	166	270	8	5	140	40	40	36	341	249
12	S	10	30	11.8	6.7	166	270	8	5	140	40	40	36	341	249
13	S	10	27	11.8	6.7	166	270	8	5	100	40	40	36	341	249
14	S	10	27	11.8	6.7	166	270	16	10	140	40	40	36	341	249
15	S	10	27	11.8	6.7	166	270	8	5	140	40	40	36	541	449
16	S	10	27	11.8	6.7	166	270	8	5	140	40	40	60	341	249
17	S	10	27	11.8	6.7	250	270	8	5	140	40	40	36	341	249
18	S	10	27	11.8	6.7	166	270	8	5	140	35	40	36	341	254
19	S	10	27	11.8	6.7	166	270	8	5	140	40	35	36	336	249
20	S	8	27	11.8	6.7	166	270	8	5	140	40	40	36	341	249

The parametric results for unstiffened extended end-plated connections are depicted in Table 8. The ratio of M_p/M_u is larger than 1.0 indicating that the extended end-plate connection reached its ultimate capacities without reaching the plastic moment capacity of the beam. The ratio of M_u/M_{pl} ranges between 1.37 and 1.57. It means that the extended end-plated connection can perform almost 1.5 times the plastic moment capacity. Similar to experimental data, a significant underestimation was observed in the ultimate capacity with an average range of 3.21 and 4.66.

Fig. 12 shows the comparison of the predicted and actual plastic moment capacities for the results of the unstiffened parametric study. The average ratios of actual plastic and predicted moment capacities are 3.83, 2.19 and 2.14 according to yield mechanisms of Srouji et al. (1983), Adey et al. (1997) and Özkılıç (2020a), respectively. For all cases, the yield mechanism of Srouji et al. (1983) significantly underestimates the plastic and ultimate moment capacity. The yield mechanisms of Adey et al. (1997) and Özkılıç (2020a) exhibited similar conservatism for both the plastic and ultimate moment capacities. Overall, the accuracy of the yield line mechanism of Özkılıç (2020a) is slightly better than that of Adey et al. (1997).

Table 9 shows the parametric results for stiffened extended end-plated connections. Similar to unstiffened case, the ratio of M_p/M_u is also larger than 1.0. The ratio of M_u/M_{pl} ranges between 1.29 and 1.57. A similar conclusion can be drawn also herein that the stiffened extended end-plated connection can perform up to almost 1.5 times plastic moment capacity. The average ratios of predicted and actual plastic moment capacities are 3.22, 2.23 and 2.22 according to the yield mechanisms of Srouji et al. (1983), Adey et al. (1997) and Özkılıç (2020a), respectively. The prediction of Özkılıç (2020a) is slightly better than the others. This can also be seen in Fig. 13. On the other hand, the average ratios of ultimate plastic and predicted moment capacities are 4.66, 3.24 and 3.21 according to yield mechanisms of Srouji et al. (1983), Adey et al. (1997) and Özkılıç (2020a), respectively. For the ultimate moment capacity, very high underestimation is also observed.

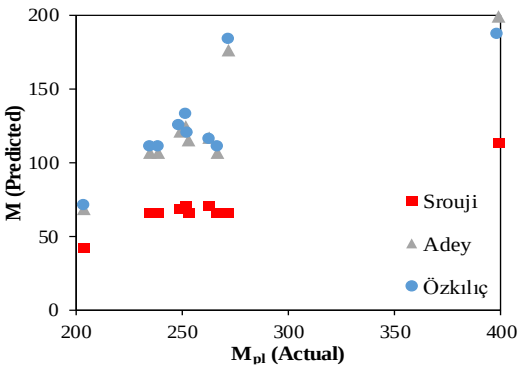

Fig. 12. The comparison of actual and predicted moment capacities for unstiffened cases.

Table 8. Results of the parametric study for unstiffened cases.

#	M_{pl}	M_u	M_p	M_p/M_u	M_u/M_{pl}	M_S	M_A	$M_{Ö}$	M_{pl}/M_S	M_{pl}/M_A	$M_{pl}/M_{Ö}$	M_u/M_S	M_u/M_A	$M_u/M_{Ö}$
1	235	349	415	1.19	1.48	66	107	111	3.54	2.19	2.12	5.25	3.25	3.14
2	253	373	415	1.11	1.47	66	116	120	3.81	2.18	2.11	5.61	3.22	3.11
3	263	372	415	1.12	1.41	71	117	116	3.72	2.25	2.28	5.26	3.17	3.22
4	272	374	415	1.11	1.37	66	177	184	4.10	1.54	1.48	5.63	2.12	2.04
5	399	614	767	1.25	1.54	114	199	187	3.50	2.00	2.13	5.40	3.08	3.28
6	239	351	415	1.18	1.47	66	107	111	3.60	2.23	2.15	5.28	3.27	3.16
7	267	400	415	1.04	1.50	66	107	111	4.02	2.49	2.41	6.03	3.73	3.61
8	249	355	415	1.17	1.43	69	121	125	3.62	2.05	1.99	5.16	2.93	2.84
9	252	358	415	1.16	1.42	70	125	133	3.59	2.01	1.90	5.10	2.86	2.70
10	204	323	415	1.28	1.59	42	69	71	4.80	2.97	2.87	7.61	4.72	4.56
Mean	263	387	450	1.16	1.47	70	125	127	3.83	2.19	2.14	5.63	3.24	3.16
Min	204	323	415	1.04	1.37	42	69	71	3.50	1.54	1.48	5.10	2.12	2.04
Max	399	614	767	1.28	1.59	114	199	187	4.80	2.97	2.87	7.61	4.72	4.56

Table 9. Results of the parametric study for stiffened cases.

#	M_{pl}	M_u	M_p	M_p/M_u	M_u/M_{pl}	M_S	M_A	$M_{Ö}$	M_{pl}/M_S	M_{pl}/M_A	$M_{pl}/M_{Ö}$	M_u/M_S	M_u/M_A	$M_u/M_{Ö}$
1	252	375	415	1.11	1.49	87	116	119	2.89	2.17	2.12	4.30	3.22	3.16
2	270	403	415	1.03	1.49	87	125	128	3.10	2.16	2.11	4.62	3.22	3.15
3	317	408	415	1.02	1.29	96	133	131	3.29	2.38	2.42	4.24	3.07	3.12
4	296	415	415	1.00	1.40	87	185	184	3.39	1.60	1.61	4.76	2.24	2.26
5	489	690	767	1.11	1.41	147	215	200	3.33	2.28	2.45	4.70	3.21	3.45
6	265	391	415	1.06	1.47	90	120	123	2.95	2.22	2.16	4.34	3.27	3.18
7	295	414	415	1.00	1.40	87	116	119	3.38	2.54	2.48	4.75	3.56	3.48
8	261	383	415	1.08	1.47	90	130	133	2.91	2.00	1.96	4.28	2.94	2.88
9	258	379	415	1.09	1.47	91	133	138	2.83	1.94	1.86	4.16	2.84	2.74
10	228	358	415	1.16	1.57	56	74	76	4.09	3.06	3.00	6.42	4.81	4.71
Mean	293	422	450	1.07	1.45	92	135	135	3.22	2.23	2.22	4.66	3.24	3.21
Min	228	358	415	1.00	1.29	56	74	76	2.83	1.60	1.61	4.16	2.24	2.26
Max	489	690	767	1.16	1.57	147	215	200	4.09	3.06	3.00	6.42	4.81	4.71

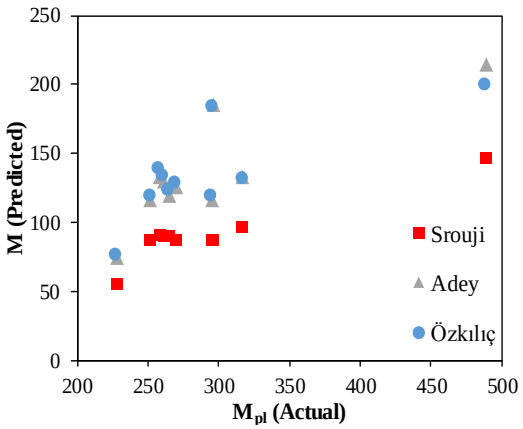

Fig. 13. The comparison of actual and predicted moment capacities for stiffened case.

6. Conclusions

In this present study, three different yield mechanisms are evaluated for both stiffened and unstiffened four bolt extended end-plated connections. Pursuant to this goal, a total of 42 experimental data is collected from 14 different studies and a parametric numerical study using ABAQUS was performed. Numerical models are capable of predicting the behavior of the extended end-plated connections. The following conclusions can be drawn based on the collected data and the parametric study:

- The prediction of plastic moment capacity by yield line mechanisms for stiffened extended end-plated connections is more accurate than that of unstiffened extended end-plated connections.

- The ultimate capacity of extended end plate connection can be averagely up to twice the plastic moment capacity.
- A general trend is observed that as the thickness of end-plate reduces, the ratio of actual moment capacities to predicted moment capacities increases. This behavior is further needed to be detailed examined.
- One should be careful about the depth of the beam while using the yield mechanism of Adey et al. (1997). If the depth of the beam is relatively high, the yield mechanism significantly overestimates the capacity.
- Numerical results revealed that the underestimation of the capacity can significantly be increased when any failure or yielding of the bolts, beam and columns is eliminated.
- The yield line mechanism proposed by Srouji underestimates the capacity. This yield mechanism is currently used by AISC 341-16 Seismic Provisions for Structural Steel Buildings with a safety factor of 0.9 which makes it more conservative.
- Among three yield mechanisms, the yield mechanism proposed by Özkılıç (2020a) gives more accurate estimation of the moment capacity. If this yield line mechanism is adopted in the guidelines (AISC 358 or TBEC 2018), it is recommended to use safety factor of 0.9 (0.9x1.67 for ASD) to predict plastic moment capacity while it is advised to utilize 1.25 (1.25x1.67 for ASD) overstrength factor to predict ultimate moment capacity.
- Based on the results of the parametric study, for future studies a new yield line mechanism to predict unstiffened and stiffened extended end-plated connections to be developed is recommended.

REFERENCES

Abel MSM, Murray TM (1994). Analytical and Experimental Investigation of the Extended Unstiffened Moment End-plate Connection with Four Bolts at the Beam Tension Flange. Jr. Department of Civil Engineering, Structures and Materials Research Laboratory, Virginia Polytechnic Institute and State University.

Adegoke IO (2009). Ductility of Thin Extended Endplate Connections. *Ph.D thesis,* University of the Witwatersrand, Johannesburg.

Adey BT, Grondin GY, Cheng JJR (1997). Behaviour of extended end plate moment connections under cyclic loading. Structural Engineering Report No. 216, Department of Civil and Environmental Engineering, University of Alberta, Edmonton, Alta.

AISC 341–16 (2016). Seismic Provisions for Structural Steel Buildings. American Institute of Steel Construction, Chicago, IL.

AISC 358–16 (2016). Prequalified Connections for Special and Intermediate Steel Moment Frames for Seismic Applications. American Institute of Steel Construction, Chicago, IL.

Akgönen Aİ, Güneş B (2017). Alın levhalı moment birleşimlerin sonlu elemanlar ile analizi. *Afyon Kocatepe Üniversitesi Fen ve Mühendislik Bilimleri Dergisi*, 17(2), 646-657. (in Turkish)

Aleksander K, Damian K (2019). Experimental tests of steel unstiffened double side joints with flush and extended end plate. *Archives of Civil Engineering*, 65(4), 127-154.

Arul Jayachandran S, Marimuthu V, Prabha P, Seetharaman S, Pandian N (2009). Investigations on the behaviour of semi-rigid endplate connections. *Advanced Steel Construction*, 5(4), 432-451.

Borgsmiller JT (1995). Simplified Method for Design of Moment End-Plate Connections, *M.Sc Thesis*, Virginia Polytechnic Institute and State University, Blacksburg, Virginia.

Borgsmiller J, Sumner E, Murray T (1995). Tests of Extended Moment End-Plate Connections Having Large Inner Pitch Distances. Research Report CE/VPI-ST-95/01 Department of Civil Engineering. Virginia Polytechnic Institute and State University. Blacksburg VA.

Bu Y, Wang Y, Zhao Y (2019). Study of stainless steel bolted extended end-plate joints under seismic loading. *Thin-Walled Structures*, *144*, 106255.

Bursi OS, Jaspart JP (1997). Calibration of a finite element model for isolated bolted end-plate steel connections. *Journal of Constructional Steel Research*, 44(3), 225-262.

Chasten CP, Lu LW, Driscoll GC (1992). Prying and shear in end-plate connection design. *Journal of Structural Engineering, ASCE*, 118(5), 1295-1311.

Coelho AMG, Bijlaard FS, da Silva LS (2004). Experimental assessment of the ductility of extended end plate connections. *Engineering Structures*, 26(9), 1185-1206.

Hendrick DM, Kukreti AR, Murray TM (1985). Unification of Flush End-Plate Design Procedures. Research Report No. FSEL/MBMA 85-01, Fears Structural Engineering Laboratory, School of Civil Engineering and Environmental Science, University of Oklahoma, Norman, Oklahoma.

Karasu A, Vatansever C (2021). Experimental study on the behavior of header end-plate connections under cyclic loading. *Teknik Dergi*, 32(6).

Kennedy NA, Vinnakota S and Sherbourne AN (1981). The split-tee analogy in bolted splices and beam-column connections. *Proceedings of the International Conference: Joints in Structural Steelwork: The Design and Performance of Semi-Rigid and Rigid Joints in Steel and Composite Structures and Their Influence on Structural Behaviour*, Teesside Polytechnic, Middlesbrough, Cleveland, England, 2.138-2.157.

Mann AP, Morris LJ (1979). Limit design of extended endplate connections. *ASCE Journal of Structural Engineering*, 105(ST3), 511–526.

Murray TM (1988). Recent developments for the design of moment end-plate connections. *Steel Beam-to-Column Building Connections*, Chen WF, ed., Elsevier Applied Science, New York, 133-162.

Murray TM (1990). AISC Design Guide 4, Extended End-Plate Moment Connections, American Institute of Steel Construction, Chicago.

Murray TM, Shoemaker WL (2002). Steel Design Guide 16, Flush and Extended Multiple-Row Moment End-Plate Connections, American Institute of Steel Construction, Chicago, IL.

Özkılıç YO (2020a). Experimental and Numerical Studies on Replaceable Links for Eccentrically Braced Frames. *Ph.D thesis*, Middle East Technical University, Ankara, Turkey.

Özkılıç YO (2020b). A new replaceable fuse for moment resisting frames: Replaceable bolted reduced beam section connections. *Steel and Composite Structures*, 35, 353-370.

Özkılıç YO (2021). Investigation of the effects of bolt diameter and end-plate thickness on the capacity and failure modes of end-plated beam-to-column connections. *Research on Engineering Structures & Material*, In-Press.

Özkılıç YO, Topkaya C (2021a). Extended end-plate connections for replaceable shear links. *Engineering Structures*, 240, 112385.

Özkılıç YO, Topkaya C (2021b). The plastic and the ultimate resistance of four-bolt extended end-plate connections. *Journal of Constructional Steel Research*, 181, 106614.

Qiang X, Wu N, Luo Y, Jiang X, Bijlaard F (2018). Experimental and theoretical study on high strength steel extended endplate connections after fire. *International Journal of Steel Structures*, 18(2), 609-634.

Packer JA, Morris LJ (1977). A limit state design method for the tension region of bolted beam column connections. *The Structural Engineer*, 55(10): 446–458.

Ryan JC (1999). Evaluation of extended end-plate moment connections under seismic loading. *Ph.D thesis,* Virginia Tech, United States.

Sağıroğlu M (2018). Kiriş gövdesinde berkitmeli alın levhalı birleşimlerin davranışının deneysel analizi. *Sakarya University Journal of Science*, 22(2), 502-508. (in Turkish)

Shi YJ, Chan SL, Wong YL (1996). Modeling for moment-rotation characteristics for end-plate connections. *Journal of Structural Engineering*, 122(11), 1300-1306.

Srouji R, Kukreti R, Murray T (1983). Yield-Line Analysis of End-Plate Connections with Bolt Force Predictions. Research Report FSEL/MBMA 83-05 Fears Structural Engineering Laboratory, University of Oklahoma, Norman OK.

Sumner EA (2003). Unified design of extended end-plate moment connections subject to cyclic loading. *Ph.D thesis,* Virginia Tech, United States.

Sumner EA, Murray TM (2001). Experimental Investigation of the MRE 1/2 End-Plate Moment Connection, Research Report No. CE/VPI-ST-01/14, submitted to Metal Building Manufacturers Association, Cleveland, Ohio.

Sumner EA, Murray TM (2002). Behavior of extended end-plate moment connections subject to cyclic loading. *Journal of Structural Engineering,* 128(4), 501-508.

Surtees J, Mann A (1970). End plate connections in plastically designed structures. C*onference on Joints in Structures: Institution of Structural Engineers,* University of Sheffield, United Kingdom.

TBEC (2018). Turkish Building Earthquake Code. Turkey Ministry of Interior Disaster and Emergency Management Authority, Ankara, Turkey.

Yılmaz O, Bekiroğlu S (2016). Alın levhalı bulonlu kolon kiriş birleşimlerinde panel bölgesi güçlendirmesinin etkisi. *Gazi Üniversitesi Mühendislik-Mimarlık Fakültesi Dergisi*, 31(2). (in Turkish)

Yun X, Gardner L (2017). Stress-strain curves for hot-rolled steels. *Journal of Constructional Steel Research*, 133, 36-46.

Wang J, Uy B, Thai HT, Li D (2018). Behaviour and design of demountable beam-to-column composite bolted joints with extended end-plates. *Journal of Constructional Steel Research*, 144, 221-235.

Whittaker D, Walpole WR (1982). Bolted end plate connections for seismically-designed steel frames. Research Report No. 82-11, Department of Civil Engineering, University of Cantebury, Christchurch, New Zealand, 88–92.

Zhu C, Rasmussen KJ, Yan S, Zhang H (2019). Experimental full-range behavior assessment of bolted moment end-plate connections. *Journal of Structural Engineering*, 145(8), 04019079.